Korean J. Chem. Eng., 37(5), 850-865 (2020)
DOI: 10.1007/s11814-020-0505-6

pISSN: 0256-1115
eISSN: 1975-7220

Separation of methanol-chloroform mixture using pressure-swing distillation: Modeling and optimization

Russel J. Galanido, Dong Sun Kim, and Jungho Cho†

Chemical Process Research Laboratory, Department of Chemical Engineering, Kongju National University, 275 Budae-dong, Cheonan-si, Seobuk-gu, Chungcheongnam-do 31080, Korea
(*Received 25 November 2019 • accepted 31 January 2020*)

Abstract−The separation of methanol-chloroform mixture, a minimum-boiling azeotrope, is performed using pressure-swing distillation process via process simulation. In this study, the steady-state optimization was carried out using PRO/II with PROVISION v.10. The two different column configurations (low-to-high pressure and high-to-low pressure) were compared wherein the positions of the low-pressure column and high-pressure column were operated interchangeably to attain an optimized design. Additionally, different heat-integration configurations (partial heat- and full heat-integration) were applied to lessen the overall utility consumption. It was determined that the low-to-high pressure column configuration provided a more optimized result for all heat-integrated systems as compared to high-to-low pressure column configuration. Application of heat-integration further decreases the cooling water and steam consumption by 38.86% and 35.74%, respectively, for partial heat-integrated system, and by 44.58% and 41.01%, respectively, for full heat-integrated system.

Keywords: Pressure-swing Distillation, Vapor-liquid Equilibrium, Methanol-chloroform, Minimum-boiling Azeotrope, Process Simulation

INTRODUCTION

Organic waste composed mainly of methanol and chloroform mixture is an effective and widely used solvent for bioactive substances extraction from biological sources in the pharmaceutical and biotechnology industry [1-4]. This binary mixture exhibits a minimum-boiling temperature azeotrope with ~65 mol% chloroform composition at ~53.4 °C under atmospheric pressure [5,6]. Thus, the mixture cannot be separated by conventional distillation columns.

There are several published works that utilized different types of special azeotropic distillation for the separation of methanol-chloroform mixture [3,7-9]. Van Kaam et al. and Langston et al. both used extractive distillation with water as the solvent [3,7]. On the other hand, Wang et al. and Hosgor et al. both applied pressure-swing distillation (PSD). The former used intelligent optimization algorithms to design and optimize the PSD process, which requires a complicated computer-encoding text to run the simulation [8]. The latter compared the separation of methanol-chloroform mixture through extractive distillation process with PSD process. In that work, we found that PSD, with or without heat-integration, has an economic advantage over extractive distillation by using the same feed information and product specifications. It is mainly due to the additional heat requirement needed for the solvent in extractive distillation. However, the optimum steady-state design is not well-established since the distillate compositions on both low- and high-pressure columns are only assumed and not optimized. Additionally, only the conventional low-to-high pressure (LP+HP) column configuration was used, and the feasibility of using high-to-low pressure (HP+LP) column configuration was not explored. Also, the advantage of partial heat-integration over other types of heat-integration schemes is not discussed [9]. Thus, a PSD process for the separation of methanol-chloroform mixture was also utilized in this study.

PSD uses two columns operating at two different pressures to separate binary azeotropic mixtures by taking high-purity product streams from one end of the columns and recycling the streams from the other end with compositions near the two azeotropes. This configuration can economical when changes in pressure significantly shift the composition of the azeotrope. PSD does not require new additive, making it an environment-friendly process. However, PSD is specifically challenging for homogeneous azeotrope separation. Some of the azeotropes that can be possibly separated by PSD are listed in Table 1 [10].

The feed information and product specifications were adapted from Hosgor et al's work to systematically compare the results from the steady-state simulation optimization.

The objectives of the study were the following: (1) to establish the most appropriate thermodynamic model for the methanol-chloroform system by evaluating various sets of experimental vapor-liquid equilibrium data obtained from the literature, (2) to determine the optimum column specifications, such as the number of theoretical stages, feed stage location, and distillate composition to minimize the total reboiler duties in the system, (3) to apply and analyze the impact of adding heat-integration in the system, and (4) to compare the results between LP+HP and HP+LP configurations as well as the simulation results based from the literature.

†To whom correspondence should be addressed.
E-mail: jhcho@kongju.ac.kr
Copyright by The Korean Institute of Chemical Engineers.

Table 1. List of binary azeotropes that can be possibly separated by PSD

No.	Components
1	Aniline - octane
2	Benzene - cyclohexane
3	Benzene - hexane
4	Benzene - isobutyl alcohol
5	Carbon dioxide – ethylene
6	Carbon tetrachloride - ethyl acetate
7	Dimethylamine - trimethylamine
8	Ethanol - benzene
9	Ethanol - dioxane
10	Ethanol - heptane
11	Methanol - acetone
12	Methanol - benzene
13	Methanol - chloroform
14	Methanol - dichloromethane
15	Methanol - ethyl acetate
16	Methanol - methyl acetate
17	Methanol - methyl ethyl ketone
18	Phenol - butyl acetate
19	1-Propanol - benzene
20	1-Propanol - cyclohexane
21	2-Propanol - benzene
22	Water - acetonitrile
23	Water - ethanol
24	Water - hydrocloric acid
25	Water - propylene oxide
26	Water - methyl acetate
27	Water - methyl ethyl ketone
28	Water - propionic acid
29	Water - propylene oxide
30	Water - tetrahydrofuran

VAPOR-LIQUID EQUILIBRIUM ANALYSIS

Isobaric vapor-liquid equilibrium (VLE) experimental data of methanol-chloroform mixture were collected from various references [11-14]. Table 2 shows the list of references for selected VLE experimental data from the literature that were subjected for analysis. The VLE experimental data were selected based on the smoothness of the generated x-y plot and T-x-y plot, which is comparable with the built-in VLE plot in PRO/II. All VLE experimental data selected were conducted at P=1.01325 bar.

The VLE experimental data were then fitted with three liquid activity (LACT) models such as the universal quasi-chemical (UNIQUAC), Wilson, and non-random two-liquid (NRTL) models, in which their corresponding built-in binary interaction parameters (Table 3) in PRO/II were used. As can be seen in Fig. 1, all the data showed good prediction with each of the LACT models. For a more precise comparison, statistical measures of dispersion, such as the average absolute deviation (AAD%), root-mean-square deviation (RMSD), and coefficient of variation of root-mean-square deviation (CV(RMSD)%), were calculated by using the experimental and calculated data. AAD%, RMSD, and CV(RMSD)% are defined by Eqs. (1) to (3), respectively, where N and y_i represent the number of data and vapor mole fraction of component *i*.

Table 3. Built-in binary interaction parameters of chloroform(i)-methanol(j) system in PRO/II

Thermodynamic model	Binary interaction parameters
UNIQUAC	A_{ij}=658.0330 A_{ji}=−137.5050
Wilson	A_{ij}=−162.7122 A_{ji}=861.7091
NRTL	A_{ij}=0 A_{ji}=0 B_{ij}=1377.24 B_{ji}=−626.018 α_{ij}=0.095

$$AAD\% = \frac{100}{N}\sum\left|y_i^{expt} - y_i^{calc}\right| \quad (1)$$

$$RMSD = \sqrt{\frac{\sum(y_i^{expt} - y_i^{calc})^2}{N}} \quad (2)$$

$$CV(RMSD)\% = \frac{RMSD}{(\sum y_i^{expt})/N} \times 100 \quad (3)$$

A summary of the calculated AAD%, RMSD, and CV(RMSD)% for each dataset is shown in Table 4. It can be observed that the calculated percent deviation for AAD and CV(RMSD) was below 5% for all datasets and thermodynamic models used. It implies that there were no significant differences between the experimental and calculated values at 95% confidence. Thus, any of the LACT models mentioned can be applied. However, the NRTL model gave the narrowest dispersion between the experimental and calculated values based on the results of datasets 1 and 2. In addition, most of the published papers pertaining to methanol-chloroform separation also used the NRTL model in their respective works [3,7-9]. Therefore, NRTL, with built-in binary interaction parame-

Table 2. List of selected vapor-liquid equilibrium experimental data from literature

Experimental data set No.	No. of points	Reference	Reference No.
1	21	Q. Li et al., *J. Chem. Eng. Data*, 2014, 59, 234-239	[11]
2	21	T. Hiaki et al., *J. Chem. Eng. Data*, 1994, 39, 714-719	[12]
3	10	I. I. Vasil'eva et al., Deposited Doc. (VINITI 3400-83), 1983	[13]
4	22	I. Nagata, *J. Chem. Eng. Data*, 1962, 7, 367-373	[14]

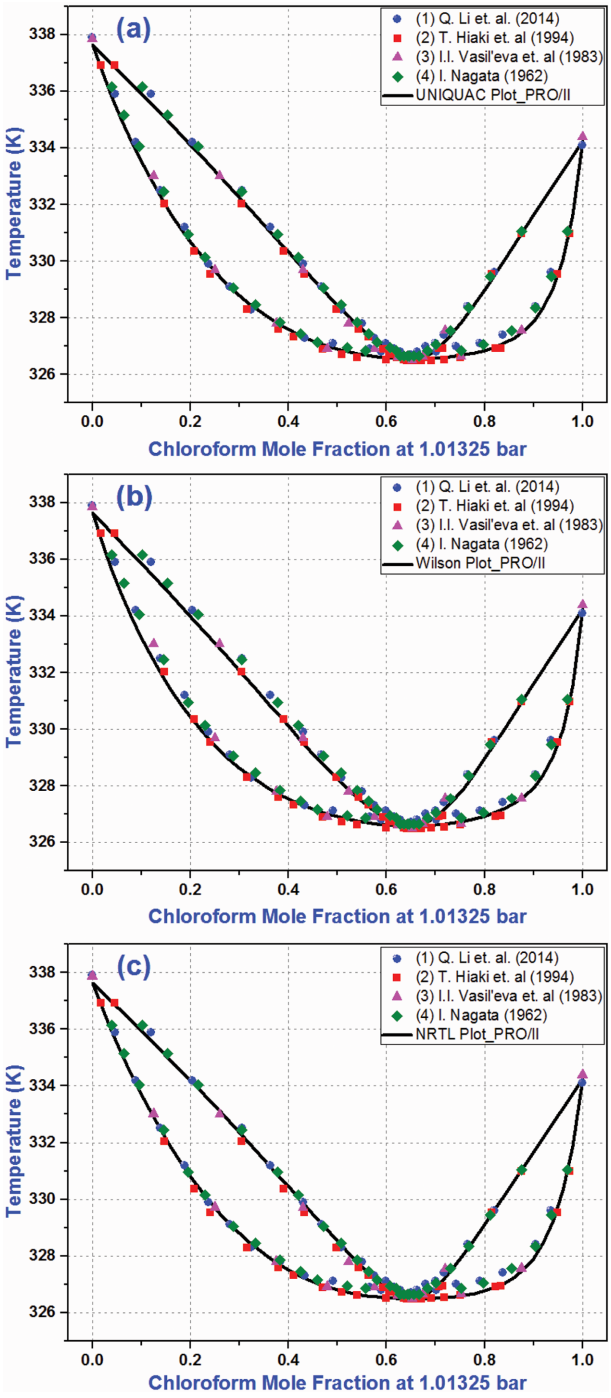


Fig. 1. T-x-y plot of VLE experimental and its prediction with (a) UNIQUAC, (b) Wilson, and (c) NRTL.

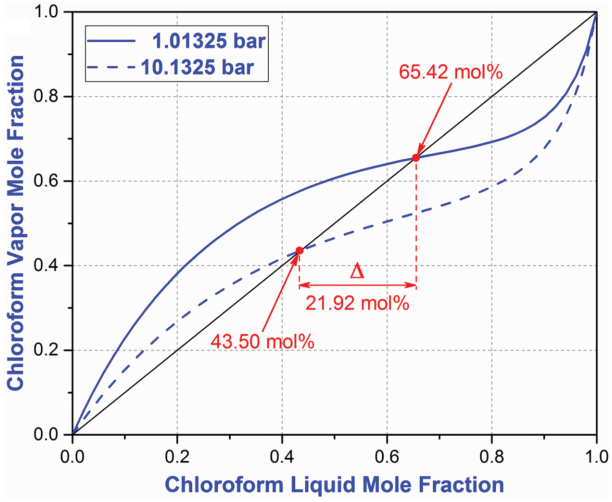


Fig. 2. x-y diagram for chloroform-methanol system at P=1.01325 bar and P=10.1325 bar.

ters, was utilized as the thermodynamic model in this study.

For this work, the operating conditions used were the same as Hosgor et al.'s work. The operating pressure applied for LP and HP columns was P=1.01325 bar and P=10.1325 bar, respectively. At P=1.01325 bar, the azeotropic composition was 65.42 mol% chloroform with a corresponding azeotropic temperature of 326.5 K. On the other hand, at P=10.1325 bar, the azeotropic composition and temperature were 43.50 mol% chloroform and 404.6 K, respectively. It can be noticed that the azeotropic point shifted from left to right when the pressure was increased from 1.01325 bar to 10.1325 bar.

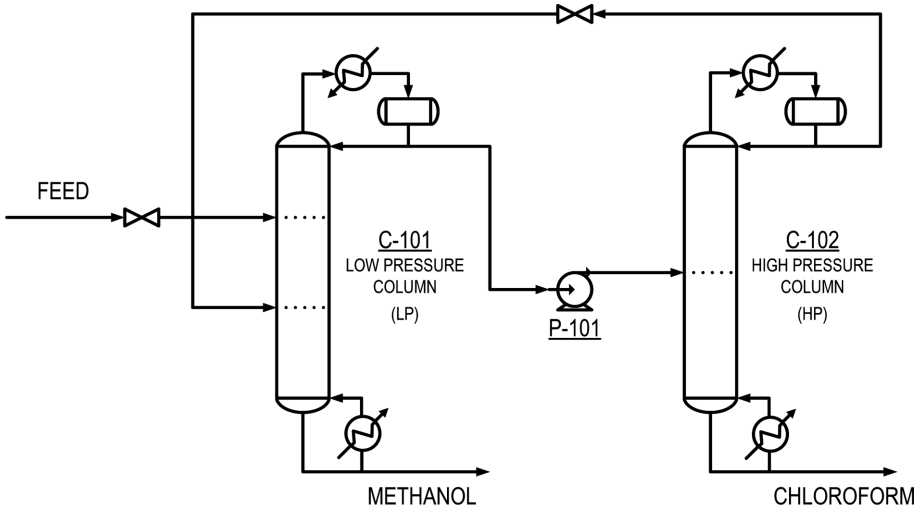
To further analyze the azeotropic shift in the system, an x-y diagram at the two different pressures was constructed. The difference between the two azeotropic points can be observed from the intersection of the equilibrium curves and diagonal lines as depicted in Fig. 2, wherein the equilibrium curve shifted from left side to the right side of the diagonal. It is apparent that the azeotropic composition moved from a low- to a high-pressure condition. The large shift in the azeotropic composition, with a difference of 21.92 mol%, indicates that separation via pressure-swing distillation is feasible for the methanol-chloroform mixture.

PROCESS SIMULATION

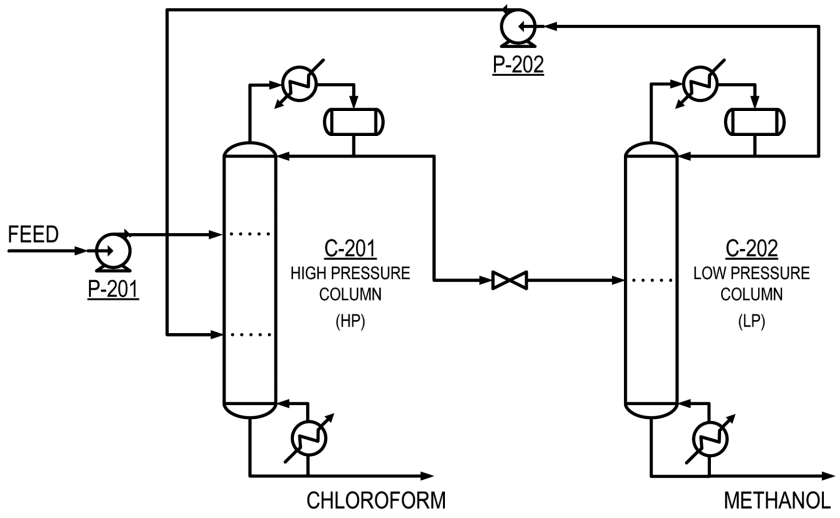
Pressure-swing distillation (PSD) uses two columns operating at two different pressures to separate binary azeotropic mixtures by taking high-purity product streams from one end of the columns

Table 4. Statistical dispersion calculation results

Expt. data set No.	UNIQUAC			Wilson			NRTL		
	AAD%	RMSD	CV(RMSD)%	AAD%	RMSD	CV(RMSD)%	AAD%	RMSD	CV(RMSD)%
1	0.4217	0.005492	1.0810	0.4612	0.005918	1.1821	0.3742	0.004688	0.9162
2	0.2844	0.003563	0.6382	0.4172	0.005188	0.9315	0.1932	0.002463	0.4336
3	0.4835	0.006085	1.1730	0.5016	0.006215	1.1987	0.4937	0.006404	1.2314
4	0.1912	0.002285	0.4524	0.3208	0.003924	0.7760	0.2300	0.002713	0.5205



(a) LP+HP Column Configuration



(b) HP+LP Column Configuration

Fig. 3. PSD process flow diagram for methanol-chloroform separation.

and recycling the streams from the other end with compositions near the two azeotropes [15,16]. Fig. 3 illustrates the PSD flow diagram for both LP+HP and HP+LP column configurations. Since the methanol-chloroform mixture exhibits minimum-boiling azeotrope, minimum-boiling distillation sequence should be employed, wherein the distillates are the circulating streams while the bottoms are the product streams for both columns.

1. Steady-state Conditions

Some of the information based on Hosgor et al's work was used for the steady-state simulation. These include the feed information, column operating pressure and pressure drop, and bottoms product specifications. All other required inputs were supplied based on existing design practices.

The feedstock characterization and product, distillation column initial specifications and operating conditions, utility conditions, and pumps and control valves outlet pressure are summarized in Table 5. For the distillate composition for the columns, the initial values were based on ±2 mol% chloroform increment on the column's azeotropic point. The values were slightly different in this study in comparison with the reference since different simulation tools were used. For the utility conditions, cooling water inlet/outlet temperatures and steam supply temperature were added to estimate the utility consumption needed for the entire process. The cooling water conditions were based on typical design practice, while the steam supply temperature should be at least 10 °C higher than the HP column bottom temperature for heat transfer [17]. Additionally, the initial values for the number of stages and feed/recycle streams were set to 25 and 13, respectively [Supplementary Fig. 1 and Supplementary Table 1].

2. Pressure-swing Distillation Optimization

The steady-state conditions presented were carried out for optimization. Specifically, the number of stages, reflux ratio, feed stage location, and distillate top concentration were further optimized in detail in this study. First, the optimum number of stages/trays for

Table 5. Steady-stated condition for PSD simulation

(a) Feed information

Parameters	Feed	
Temperature (K)	300.0	
Pressure (bar)	2.0265	
Vapor fraction, mole (-)	0.0	
Total molar rate (kmol/h)	100.0	
Composition	kmol/h	mol%
Chloroform	50.0	50.0
Methanol	50.0	50.0

(b) Initial column specifications and operating conditions

Specifications	Low-pressure column	High-pressure column
Pressure	1.01325 bar	10.1325 bar
Number of stages[a]	25	25
Feed/recycle stream location	13	13
Column pressure drop	0.10133 bar	0.10133 bar
Condenser outlet temperature	at Bubble Temp.	at Bubble Temp.
Azeotropic point	65.42 mol% chloroform	43.50 mol% chloroform
Distillate composition[a]	63.42 mol% chloroform	45.50 mol% chloroform
Bottoms composition	99.50 mol% methanol	99.50 mol% chloroform

(c) Utility conditions

Utility	Temperature (°C)
Steam supply	180 (Saturated)
Cooling water supply	32
Cooling water return	40

(d) Pumps and control valves outlet pressure

Equipment	Outlet pressure (bar)
Pumps	11.14575
Feed control valves	1.01325/10.1325[b]
Product control valves	1.01325/10.1325[c]

[a]Initial values subjected for optimization.
[b]Depending on the downstream column's pressure.
[c]P=1.01325 bar for methanol product, P=10.1325 bar for chloroform.

each column was determined. After which, the optimum feed stage location determination followed by the column distillate concentration optimization was then executed. The reflux ratio value will just float according to the optimized specifications. For all the specifications to be optimized, the objective function was to minimize the total column reboiler duties.

2-1. Number of Theoretical Stages

The number of theoretical stages optimization was based on Luyben and Chien's work [18,19]. The design was optimized using heuristics. Rigorous simulations were run with an increasing number of stages until the reflux ratio stopped decreasing or until a non-convergent simulation existed, which gives an approximation of the minimum reflux ratio. Once the approximate minimum reflux ratio was determined, the number of theoretical stages required for reflux ratio about 1.2 times of the minimum were used. For the sequence of which column will be first optimized, the column which intakes both the fresh feed and recycle stream should govern.

2-2. Feed Stage Location

The feed stage location in each column was varied to determine the ideal location that will minimize the total energy consumption of the column reboilers. Since there are three streams to be located, there are $(N_1-2)^2$ x (N_2-2) number of unique ways to arrange the location of the streams in order to know the ideal stage of each feed simultaneously. N refers to the number of stages in the column; e.g., for a pressure-swing distillation having 25 theoretical stages in both low-and high-pressure column it will have $(25-2)^2$ x $(25-2)$=12,167 ways to arrange it. Thus, it is not recommended to locate all the feed stream simultaneously. Sequential arrangement based on governing stream should be done to more simplify the process. As suggested, the feed stream(s) of the governing column should be prioritized. The leftmost column on the PSD diagram is always the governing column since it receives both the feed and the recycle streams. Between these two streams, the recycle stream should be given more priority than the fresh feed stream

since the former is expected to have a larger flow rate over the latter. After which, the feed stream entry to the non-governing column will then be optimized.

2-3. Column Distillate Concentration

The column distillate concentration optimization was derived by Cho and Jeon [20]. The concentration of distillate in each column was varied to minimize the total reboiler heat duties. In here, the chloroform concentration on the top of each column was manipulated between near the azeotropic point and the concentration corresponding to the minimum column reflux ratio with increments of 0.01 mol%. The optimum chloroform concentration on the top was individually determined on each column, starting from the governing column. Since varying the distillate concentration will also vary the column's reflux ratio, it is important to set the minimum column reflux ratio to 0.10 in cases where optimal point is not achieved.

3. Heat-integration

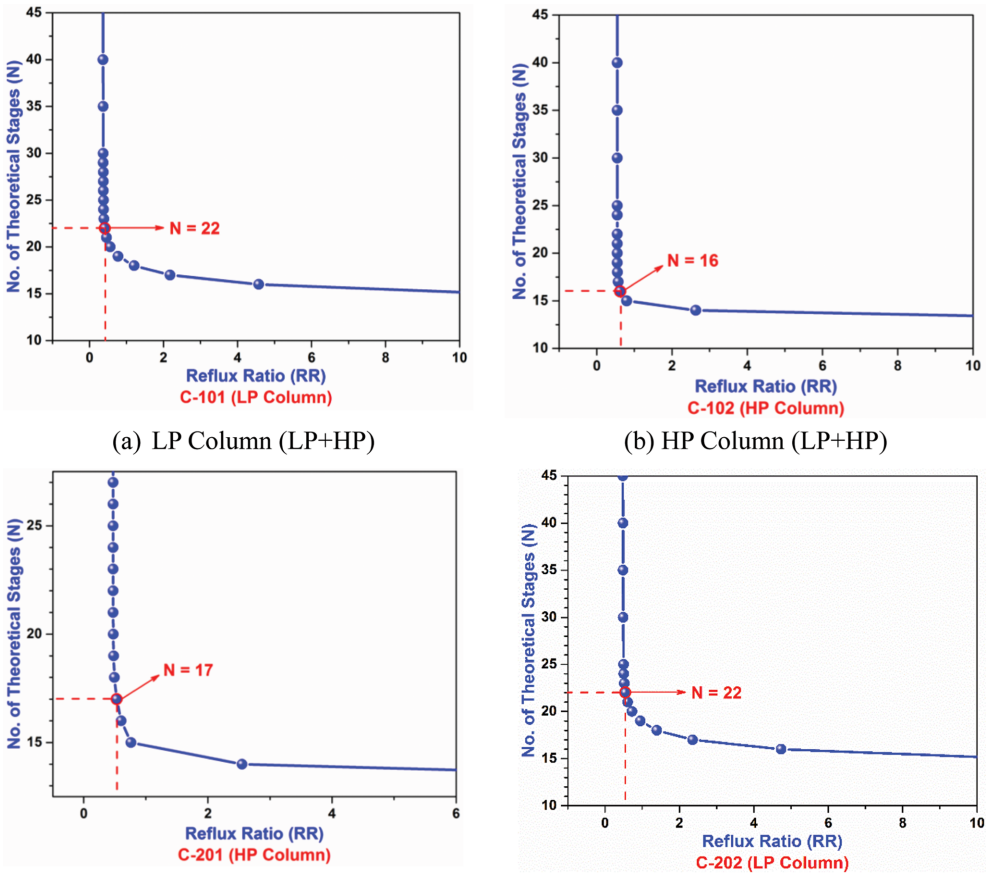
Pressure-swing distillation operates using two distillation columns at two different pressures. The difference in pressure yields a lower temperature in the LP column and a higher temperature in the HP column. When the temperature at the top of the HP column has enough drive to supply heat in the LP column reboiler, heat-integration is recommendable. The application of heat-integration is economically attractive, especially in pressure-swing distillation; where energy consumption is quite high, it lessens the overall utility consumption.

Heat-integrated systems can be considered for complete heat-integration where there is only one steam-heated reboiler and one water-cooled condenser in the HP and LP column, respectively. There is another heat exchanger that serves as the condenser for the high-pressure column and the reboiler for the LP column having process fluid on both the condensing and boiling sides. Therefore, the heat elimination in the condenser of the HP column is precisely equal to the heat input in the reboiler of the LP column.

On the other hand, heat-integrated systems can be considered for partial heat-integration where the HP condenser heat removal is not equal to the LP reboiler heat contribution. The use of auxiliary condenser and/or auxiliary reboiler is necessary.

3-1. Partial Heat-integration

The results from no heat-integration pressure-swing distillation were retained. The only difference was the further minimization of reboiler duties due to the heat-integration between HP column condenser and LP column reboiler. If the HP column condenser duty is greater than the LP column reboiler duty, an additional condenser (auxiliary condenser) at the top of HP column is necessary. If the LP column reboiler duty is greater than the HP column condenser duty, an additional reboiler (auxiliary reboiler) at the bottom of the LP column is necessary. The duty required for the auxiliary



(a) LP Column (LP+HP) (b) HP Column (LP+HP)

(c) HP Column (HP+LP) (d) LP Column (HP+LP)

Fig. 4. Number of theoretical stages (N) and reflux ratio (RR) relationship.

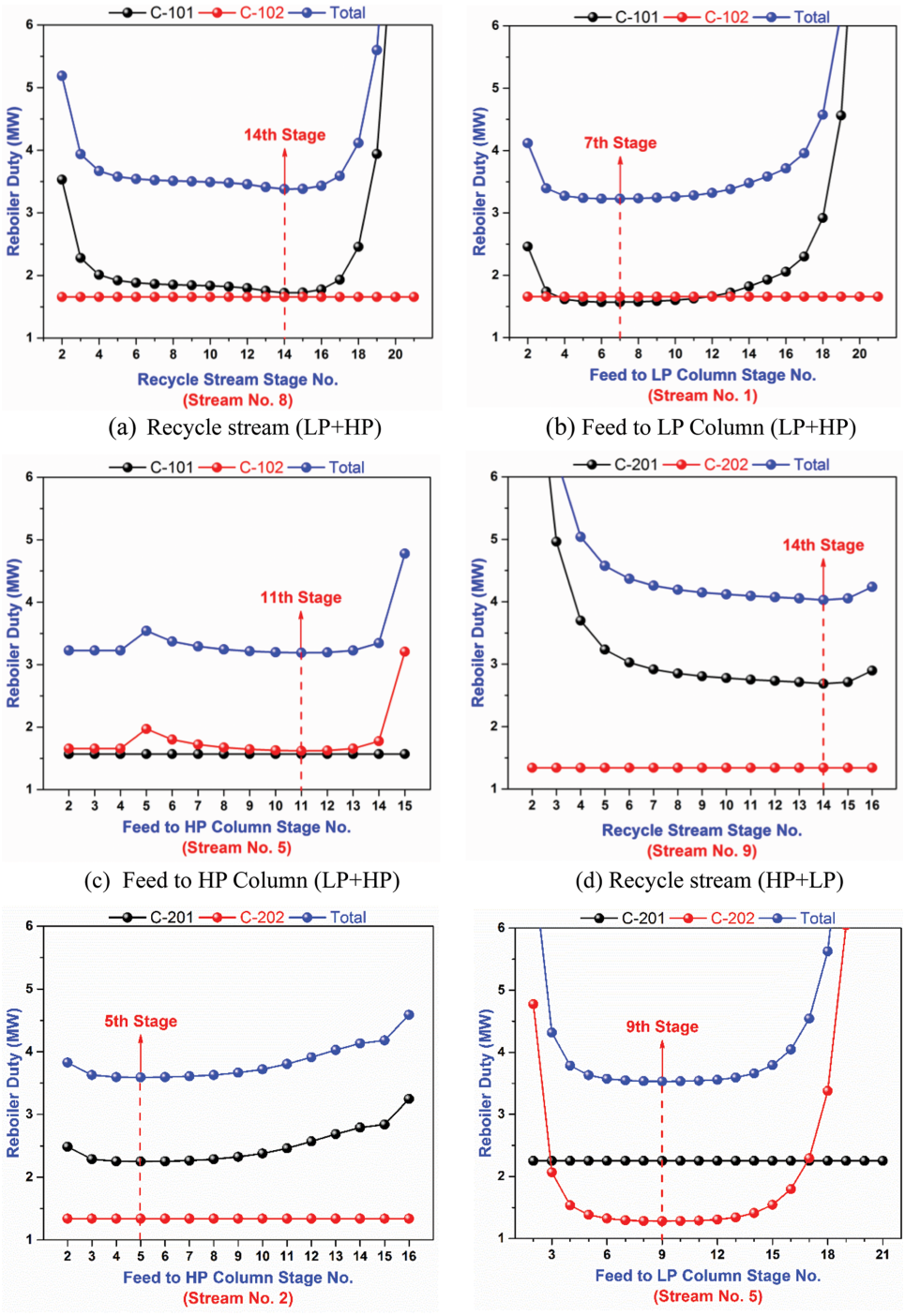
heat exchanger is equal to the absolute duty difference between HP column condenser and LP column reboiler.

3-2. Full Heat-integration

The column tray number and feed specification on each column based on no heat-integration results were retained. The LP column reboiler duty is defined as equal as the HP column condenser duty. Due to the decrease in the degree of freedom in the LP column, new optimum distillate concentration for HP column should be determined. The objective function this time was to minimize the reboiler duty of HP column.

RESULTS AND DISCUSSION

The analysis and optimization of the separation method through PSD were performed using a process simulator (PRO/II v. 10). The simulation results for PSD with different types of configurations and



(a) Recycle stream (LP+HP)

(b) Feed to LP Column (LP+HP)

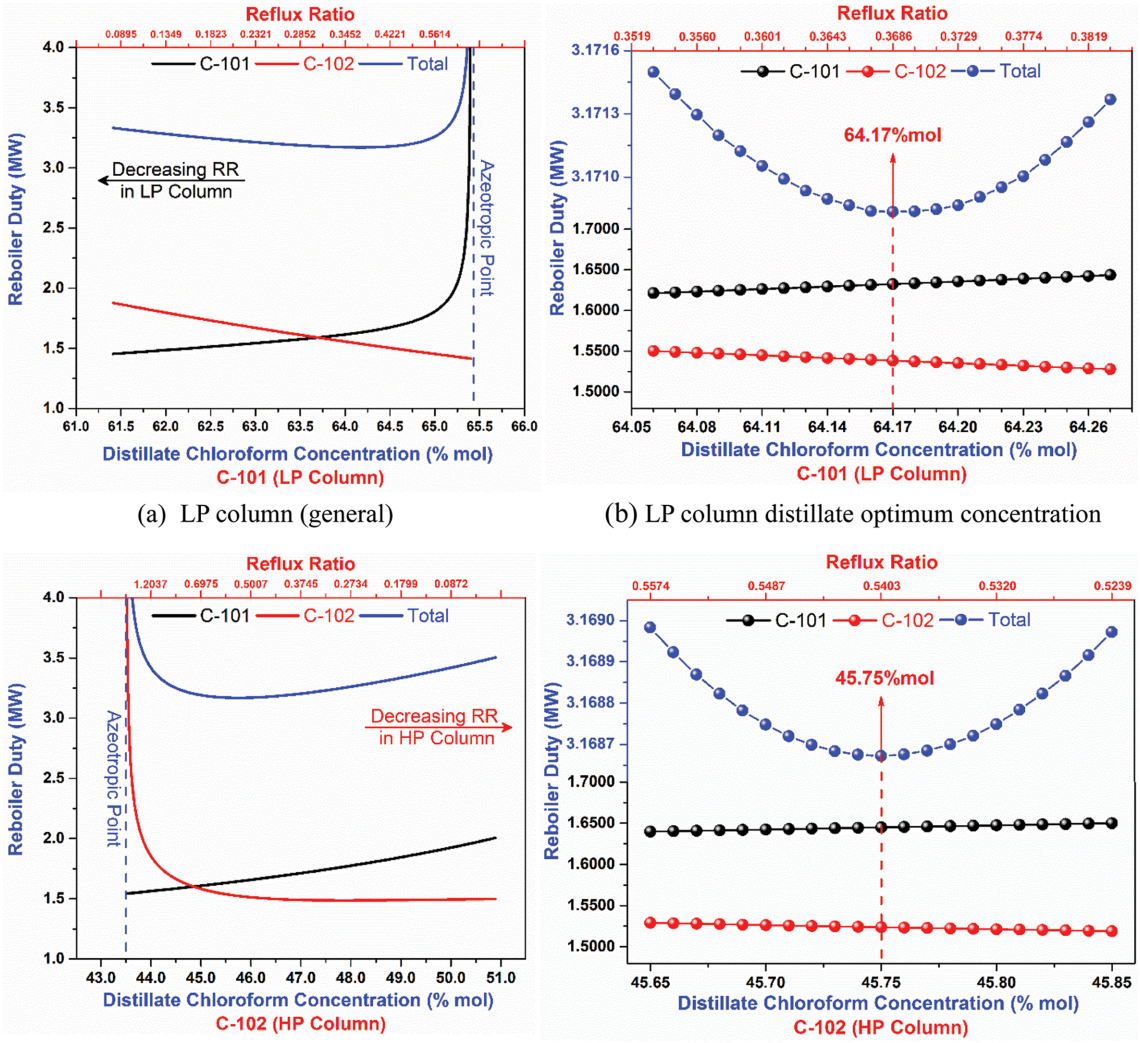
(c) Feed to HP Column (LP+HP)

(d) Recycle stream (HP+LP)

(e) Feed to HP Column (HP+LP)

(d) Feed to LP Column (HP+LP)

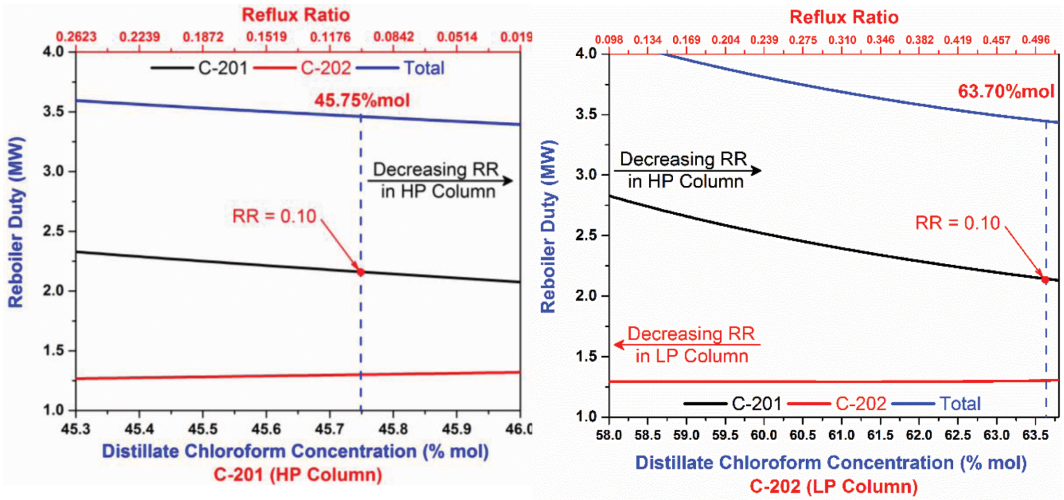
Fig. 5. Stream entry location variation and effects with all reboilers.



(a) LP column (general) (b) LP column distillate optimum concentration

(c) HP column (general) (d) HP column distillate optimum concentration

Fig. 6. Distillate concentration variation and effects with all reboiler duties in LP+HP configuration.



(a) HP column (b) LP column

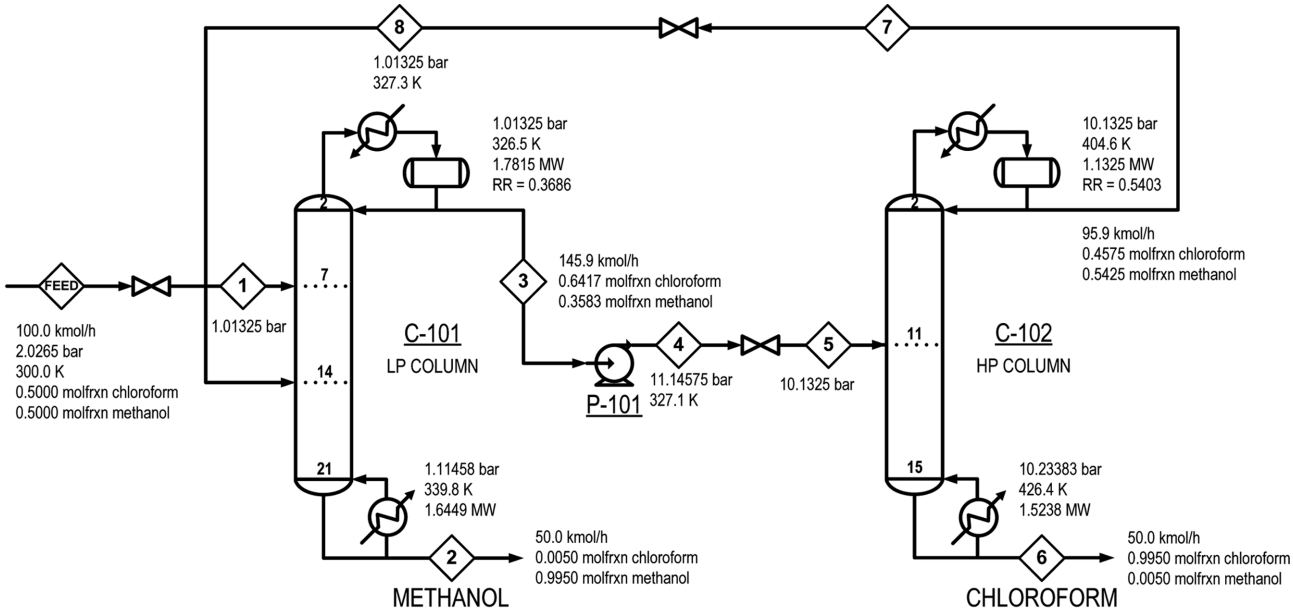
Fig. 7. Distillate concentration variation and effects with all reboiler duties in HP+LP configuration.

heat-integrations were summarized and discussed as follows.

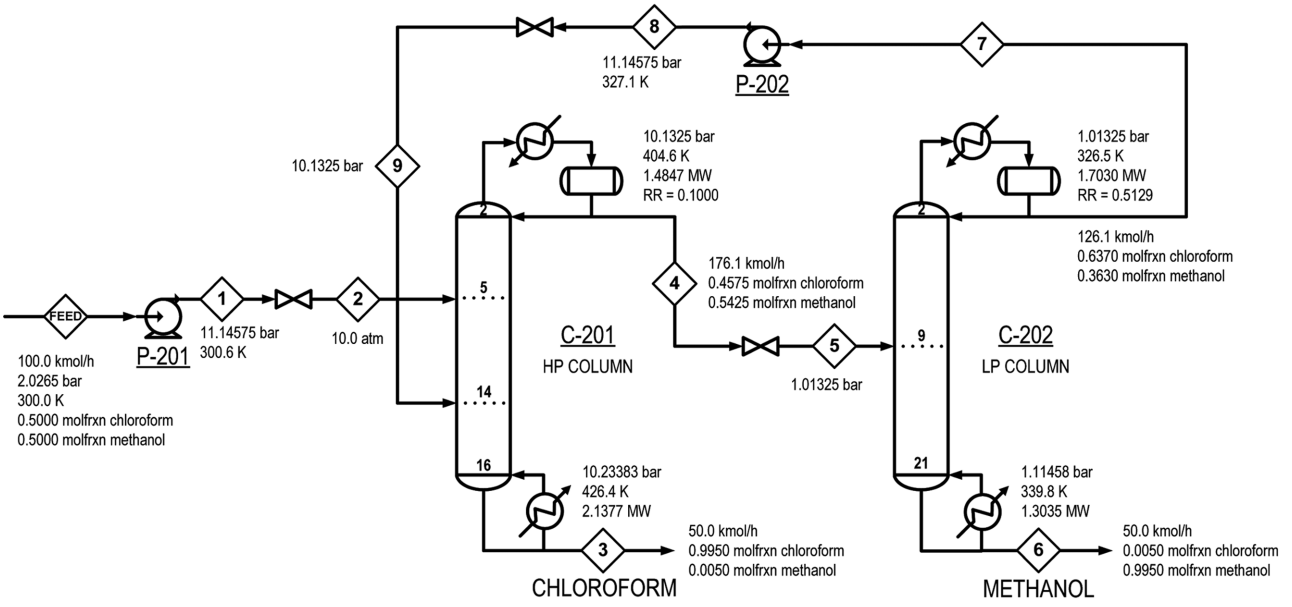
1. Pressure-swing Distillation Optimization

Pressure-swing distillation steady-state process was optimized by determining the optimum column specifications of the ff.: (1) number of theoretical trays, (2) feed stage location, and (3) column distillate composition.

For LP+HP column configuration, upon the variation of the number of theoretical stages for LP (C-101) and HP (C-102) columns at fixed initial column distillate composition, it was found out that the optimum number of stages was 22 and 16 for LP and HP column, respectively (Figs. 4(a) and 4(b), Supplementary Tables 2(a) & 2(b)). The entry location for the recycle and feed streams for LP column was determined to be at 14th and 7th stage, respectively, while the feed stream for HP column was at the 11th stage of C-102 (Figs. 5(a)-5(c)). The combination of the entry locations of the feed/recycle streams resulted in more diminished total reboiler duties. These duties were further minimized by adjusting the distillate composition at the columns in which it was found that the



(a) LP+HP Column Configuration



(b) HP+LP Column Configuration

Fig. 8. Flowsheet of optimized pressure-swing distillation with the corresponding design conditions and specifications.

optimum chloroform concentration at the top of LP and HP columns was 64.17 mol% and 45.75 mol%, respectively (Fig. 6).

On the other hand, for HP+LP column configuration, the number of theoretical stages was determined to be 17 and 22 for HP (C-201) and LP (C-202) column, respectively (Figs. 4(c) and 4(d), Supplementary Tables 2(c) and 2(d)). The recycle stream, feed to C-201, and feed to C-202 location was established to be at the 14th, 5th, and 9th stage, respectively, on their corresponding column (Figs. 5(d)-5(f)). No optimum point was observed for the chloroform concentration at the top of the HP and LP columns. The distillate composition was based at the point where the reflux ratio at HP column was 0.10, giving 45.75 and 63.70 chloroform mol% at the top of C-201 and C-202, respectively (Fig. 7).

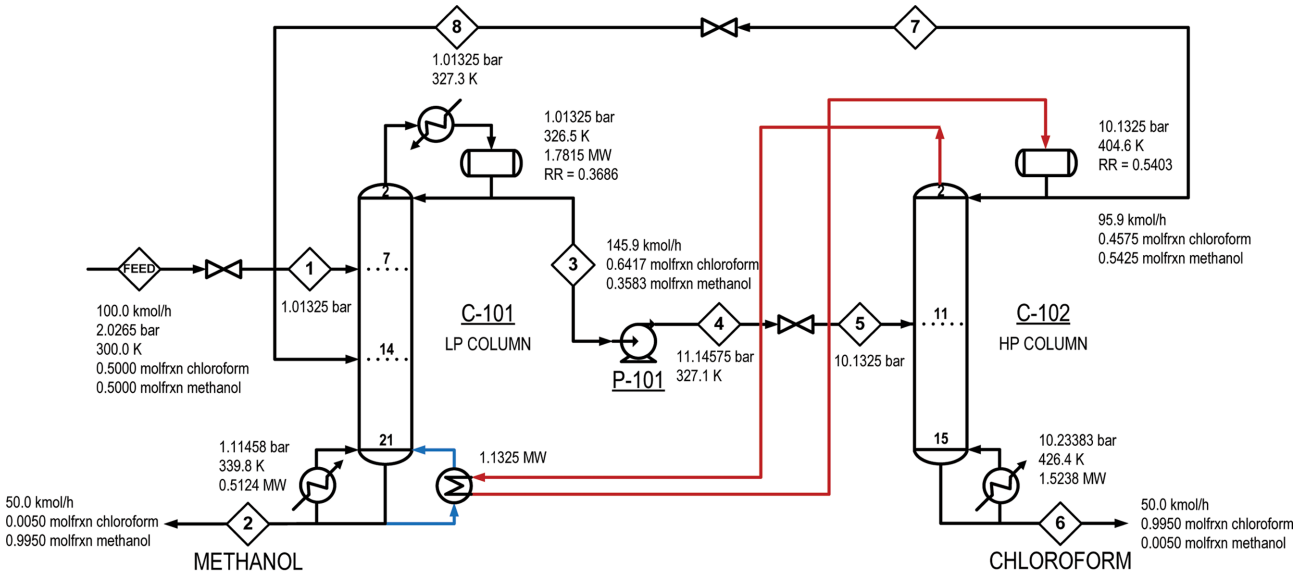
The flowsheet of the overall pressure-swing distillation process for the two column configurations was drawn to systematically analyze the simulation results, as illustrated in Fig. 8. The flowsheet shows the stream composition, optimum column specifications, and condenser and reboiler heat duty.

2. Heat-integration

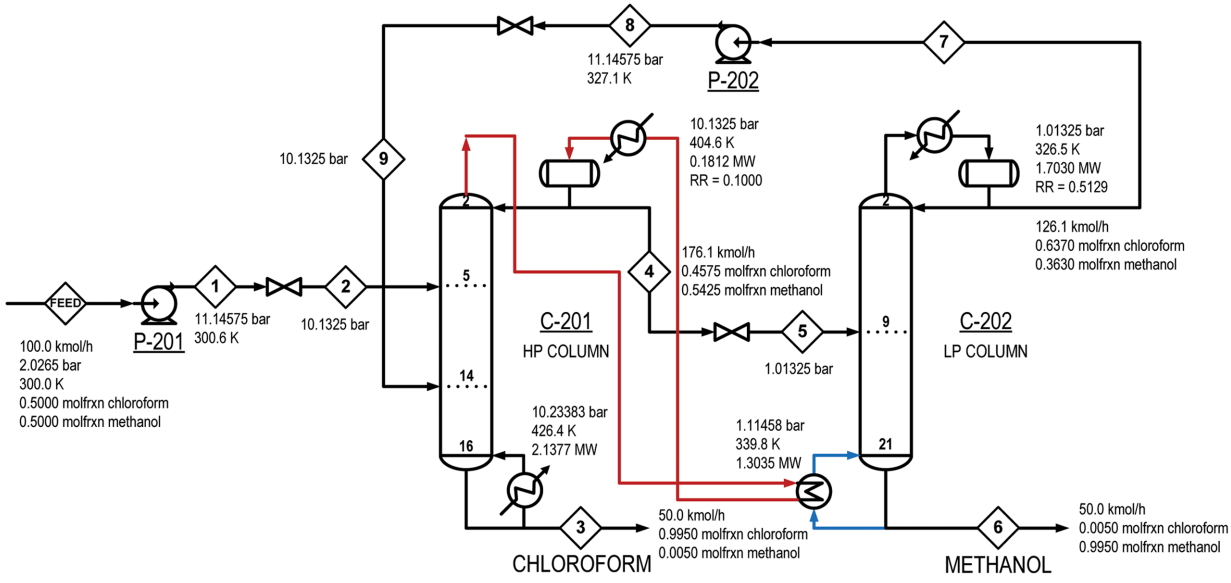
Partial and full heat-integration was applied by using an integrated heat exchanger which serves as the reboiler for the LP column and as the condenser for HP column.

2-1. Partial Heat-integration

For partial heat-integration, the results from pressure-swing dis-



(a) LP+HP Column Configuration



(b) HP+LP Column Configuration

Fig. 9. Flowsheet of optimized pressure-swing distillation with partial heat-integration including the corresponding design conditions and specifications.

tillation with no heat-integration were retained. The only difference is the further minimization of reboiler duties due to the heat-integration between HP column condenser and LP column reboiler. For LP+HP column configuration, the auxiliary reboiler was added to supply the remaining heat required not covered by the integrated heat exchanger since the LP column reboiler duty was larger than HP column condenser duty. On the other hand, for HP+LP configuration, an auxiliary condenser was added since the LP column reboiler duty was smaller than HP column condenser duty. Fig. 9 depicts the flowsheet of the pressure-swing distillation process with partial heat-integration including the corresponding design conditions and specifications. The heat duty of the integrated heat exchanger and auxiliary exchanger was also specified in the flowsheet.

Since the main purpose of heat-integration is to decrease the utility consumption (steam and cooling water flow requirement), such

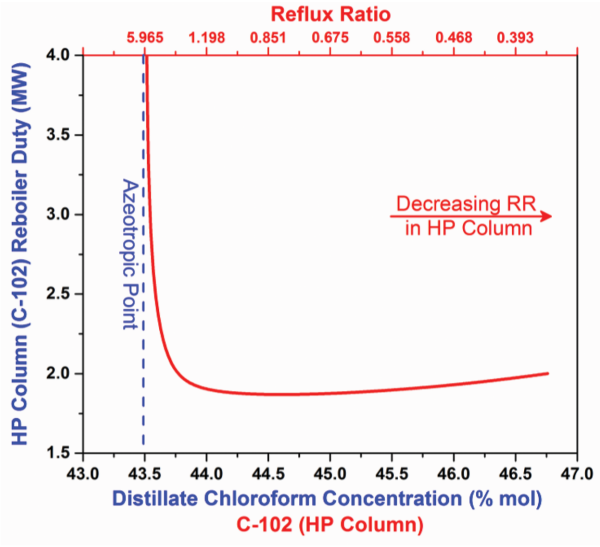
Table 6. Comparison of heat duty and utility consumption of all heat-integration systems for pressure-swing distillation

(a) LP+HP column configuration

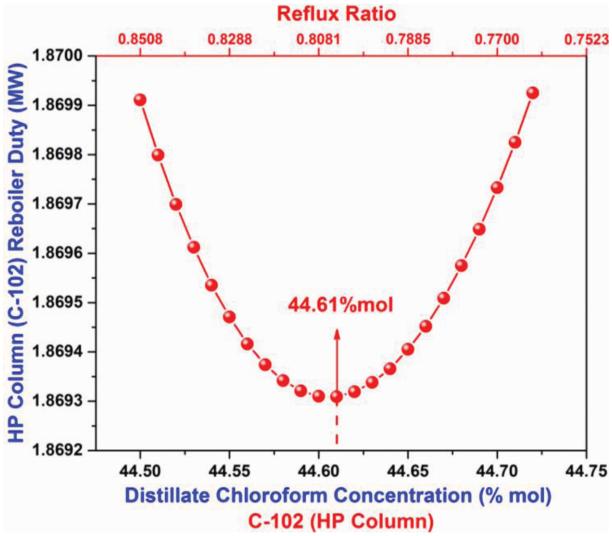
	No heat-integration	Partial heat-integration	Full heat-integration
Heat duty requirement (MW)			
LP column condenser	1.7815	1.7815	1.6148
HP column condenser	1.1325	-	-
Integrated heat exchanger	-	1.1325	1.4569
LP column reboiler	1.6449	0.5124	-
HP column reboiler	1.5238	1.5238	1.8693
Total condenser duty (MW)	**2.9140**	**1.7815**	**1.6148**
Total reboiler duty (MW)	**3.1687**	**2.0362**	**1.8693**
Cooling water req'd (mton/h)			
LP column condenser	191.48	191.48	173.56
HP column condenser	121.72	-	-
Steam requirement (kg/h)			
LP column reboiler	2938.75	915.42	-
HP column reboiler	2722.46	2722.46	3339.33
Total cooling water (mton/h)	**313.20**	**191.48**	**173.56**
Total steam req'd (kg/h)	**5661.21**	**3637.88**	**3339.33**
CW consumption reduction	-	**38.86%**	**44.58%**
Steam consumption reduction	-	**35.74%**	**41.01%**

(b) HP+LP column configuration

	No heat-integration	Partial heat-integration	Full heat-integration
Heat duty requirement (MW)			
LP column condenser	1.7030	1.7030	1.7849
HP column condenser	1.4847	0.1812	-
Integrated heat exchanger	-	1.3035	1.4072
LP column reboiler	1.3035	-	-
HP column reboiler	2.1377	2.1377	2.0386
Total condenser duty (MW)	**3.1877**	**1.8842**	**1.7849**
Total reboiler duty (MW)	**3.4412**	**2.1377**	**2.0386**
Cooling water req'd (mton/h)			
LP column condenser	183.04	183.04	191.85
HP column condenser	159.58	19.48	-
Steam requirement (kg/h)			
LP column reboiler	2328.61	-	-
HP column reboiler	3818.85	3818.85	3641.81
Total cooling water (mton/h)	**342.62**	**202.52**	**191.85**
Total steam req'd (kg/h)	**6147.46**	**3818.85**	**3641.81**
CW consumption reduction	-	**40.89%**	**44.01%**
Steam consumption reduction	-	**37.88%**	**40.76%**



(a) General



(b) Distillate optimum concentration

Fig. 10. HP column (C-102) distillate concentration variation and effect with its reboiler duty in LP+HP configuration for pressure-swing distillation with full heat integration.

utility requirements were compared to the non-heat integrated system. The summary of heat duty/utility consumptions and comparison between the pressure-swing distillation without heat-integration and with partial heat-integration are tabulated in Table 6. It was found that the total steam and cooling water requirement was reduced by 35.74% and 38.86%, respectively, for LP+HP column configuration, while 37.88% and 40.89%, for HP+LP column configuration, respectively, as compared to their non-heat integrated counterparts.

2-2. Full Heat-integration

For full heat-integration, the column tray number and feed specification on each column based on non-heat integrated system results were retained. LP column reboiler duty was defined as equal as the HP column condenser duty. Due to the decrease in the degree of

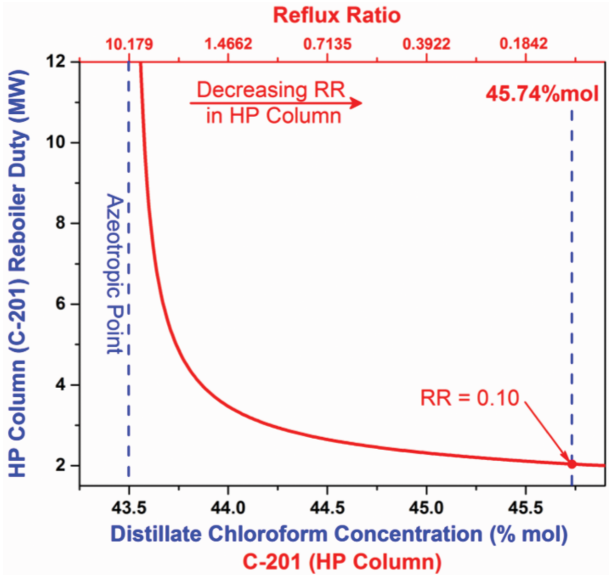


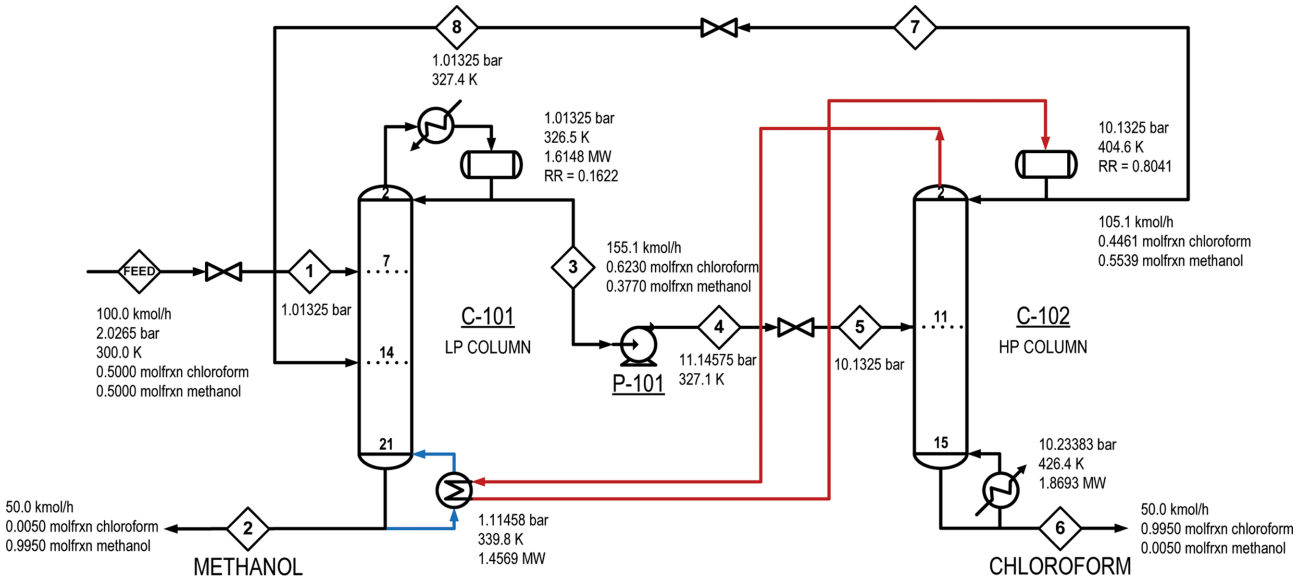
Fig. 11. HP column (C-201) distillate concentration variation and effect with its reboiler duty in HP+LP configuration for pressure-swing distillation with full heat integration.

freedom in the LP column, a new optimum distillate concentration for HP column was determined to minimize its reboiler duty. For LP+HP column configuration, the optimum distillate chloroform composition was determined to be 44.61 mol% at HP column (Fig. 10). For HP+LP column configuration, no optimum point was found, instead, the HP column reboiler duty decreases with decreasing reflux ratio. Thus, distillate composition was based at the point where the reflux ratio at HP column was 0.10, giving 45.74 chloroform mol% at the top of C-202 (Fig. 11). The flowsheet of the overall pressure-swing distillation with full heat-integration process for the two column configurations was drawn to systematically analyze the simulation results, as illustrated in Fig. 12. The flowsheet shows the stream composition, optimum column specifications, integrated heat exchanger, condenser and reboiler heat duty.

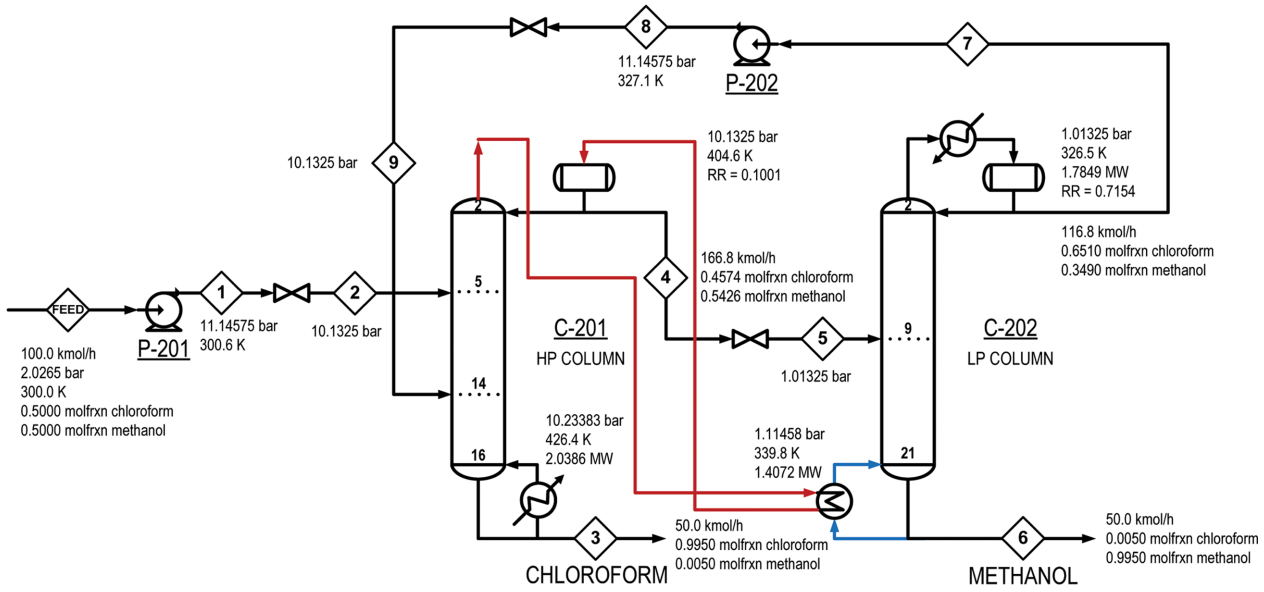
A summary of heat duty/utility consumptions and comparison between the pressure-swing distillation without heat-integration and with full heat-integration are in Table 6. It was found that the total steam and cooling water requirement was reduced by 41.01% and 44.58%, respectively, for LP+HP column configuration, while 40.76% and 44.01%, for HP+LP column configuration, respectively, as compared to their non-heat integrated counterparts.

3. Overall Comparison of Steady-state Simulation Results

The overall steady-state simulation results of pressure-swing distillation (PSD) were compared and matched against Hosgor's work, as shown in Tables 7 and 8 for non-heat integrated and fully-heat integrated system. Given that the feed information and product specifications in this study were the same as Hosgor's, the design results among results were slightly different. Hosgor's design used a greater number of theoretical stages for both LP and HP column than this work's optimized PSD design using two configurations. For PSD with no heat integration, despite the fact that the number of stages was lesser, LP+HP column configuration gave smaller condenser and reboiler duties for both columns than that of Hos-



(a) LP+HP Column Configuration



(b) HP+LP Column Configuration

Fig. 12. Flowsheet of optimized pressure-swing distillation with full heat-integration including the corresponding design conditions and specifications.

gor's design. In addition, the column inside diameter (ID) for both columns as calculated in Aspen Plus was also less. On the other hand, for PSD with full heat integration, since the number of stages was fewer, Hosgor's design calculated smaller reboiler and heat duties and column ID as compared to this work with LP+HP column configuration. However, the differences were only minimal. The increase in terms of percentage is as follows: 2.54% for condenser duty, 1.63% for reboiler duty, and 5.95% for HP column ID (LP column ID was the same). In all systems, HP+LP column configuration gave less satisfactory results as compared to LP+HP column configuration of this work and Hosgor's work.

CONCLUSIONS

Vapor-liquid equilibrium analyses and steady-state simulations for pressure-swing distillation have been presented for the separation of methanol-chloroform mixture. The thermodynamic model suited for the system can be any of the three liquid activity models (UNIQUAC, Wilson, and NRTL) analyzed in this work. Among the models, the NRTL model gave the best curve fit among the models based on data regression analysis results. The results of steady-state simulations for pressure-swing distillation process show that LP+HP column configuration is significantly more economical than

Table 7. Comparison of Hosgor et al. and optimized non-heat integrated PSD using two column configurations

	E. Hosgor et al., 2014	This work	
Column configuration	LP+HP	LP+HP	HP+LP
Thermodynamic system	NRTL	NRTL	NRTL
LP column			
Column pressure (bar)	1.01325	1.01325	1.01325
Column pressure drop (bar)	0.10133	0.10133	0.10133
N stage	24	22	22
Feed stage			
Feed	9	7	9
Recycle	18	14	-
Reflux ratio	0.55	0.37	0.51
Column diameter (m)	1.08	1.07	1.03
Heat duty			
Condenser duty (MW)	1.83	1.78	1.70
Reboiler duty (MW)	1.69	1.64	1.30
Distillate			
Temperature (K)	327.0	326.5	326.5
Flowrate (kmol/h)	134.5	145.9	126.1
Composition, mole			
Chloroform	0.64	0.64	0.64
Methanol	0.36	0.36	0.36
Bottoms			
Temperature (K)	341.1	339.8	339.8
Flowrate (kmol/h)	50.0	50.0	50.0
Composition, mole			
Chloroform	0.005	0.005	0.005
Methanol	0.995	0.995	0.995
HP column			
Column pressure (bar)	10.1325	10.1325	10.1325
Column pressure drop (bar)	0.10133	0.10133	0.10133
N stage	25	16	17
Feed stage			
Feed	20	11	5
Recycle	-	-	14
Reflux ratio	0.95	0.54	0.10
Diameter (m)	0.84	0.81	0.97
Heat duty			
Condenser duty (MW)	1.25	1.13	1.48
Reboiler duty (MW)	1.66	1.52	2.14
Distillate			
Temperature (K)	405.5	404.6	404.6
Flowrate (kmol/h)	80.2	95.9	176.1
Composition, mole			
Chloroform	0.43	0.46	0.46
Methanol	0.57	0.54	0.54
Bottoms			
Temperature (K)	426.6	426.4	426.4
Flowrate (kmol/h)	50.0	50.0	50.0
Composition, mole			
Chloroform	0.995	0.995	0.995
Methanol	0.005	0.005	0.005

Table 8. Comparison of Hosgor et al. and optimized fully-heat integrated PSD using two column configurations

	E. Hosgor et al., 2014	This work	
Column configuration	LP+HP	LP+HP	HP+LP
Thermodynamic system	NRTL	NRTL	NRTL
LP column			
Column pressure (bar)	1.01325	1.01325	1.01325
Column pressure drop (bar)	0.10133	0.10133	0.10133
N stage	24	22	22
Feed stage			
Feed	9	7	9
Recycle	18	14	-
Reflux ratio	0.30	0.16	0.72
Column diameter (m)	1.03	1.03	1.07
Heat duty			
Condenser duty (MW)	1.57	1.61	1.78
Reboiler duty (MW)	-	-	-
Distillate			
Temperature (K)	326.9	326.5	326.5
Flowrate (kmol/h)	138.1	155.1	116.8
Composition, mole			
Chloroform	0.63	0.62	0.65
Methanol	0.37	0.38	0.35
Bottoms			
Temperature (K)	337.5	339.8	339.8
Flowrate (kmol/h)	50.0	50.0	50.0
Composition, mole			
Chloroform	0.005	0.005	0.005
Methanol	0.995	0.995	0.995
HP column			
Column pressure (bar)	10.1325	10.1325	10.1325
Column pressure drop (bar)	0.10133	0.10133	0.10133
N stage	25	16	17
Feed stage			
Feed	20	11	5
Recycle	-	-	14
Reflux ratio	1.13	0.80	0.10
Diameter (m)	0.84	0.89	0.95
Heat duty			
Condenser duty (MW)	-	-	-
Reboiler duty (MW)	1.84	1.87	2.04
Distillate			
Temperature (K)	405.5	404.6	404.6
Flowrate (kmol/h)	88.1	105.1	166.8
Composition, mole			
Chloroform	0.43	0.45	0.46
Methanol	0.57	0.55	0.54
Bottoms			
Temperature (K)	426.0	426.4	426.4
Flowrate (kmol/h)	50.0	50.0	50.0
Composition, mole			
Chloroform	0.995	0.995	0.995
Methanol	0.005	0.005	0.005

HP+LP column configuration. For pressure-swing distillation with no heat-integration, despite the fact that the number of stages was less, the LP+HP column configuration gave smaller condenser and reboiler duties for both columns than that of Hosgor's design. On the other hand, for pressure-swing distillation with full heat-integration, since the number of stages was fewer, Hosgor's design calculated smaller reboiler and condenser heat duties as compared to this work with LP+HP column configuration. However, the differences were only minimal. This work also shows that using heat-integration at the design stage of the pressure-swing distillation process results in a decrease of both the capital and energy costs.

ACKNOWLEDGEMENT

This work was supported by the research grant of the Kongju National University in 2019.

CONFLICT OF INTEREST

The authors declare that there is no conflict of interest regarding the publication of this manuscript.

SUPPORTING INFORMATION

Additional information as noted in the text. This information is available via the Internet at http://www.springer.com/chemistry/journal/11814.

REFERENCES

1. C. L. Schengrund and P. Kovac, *J. Lipid Res.*, **40**, 160 (1999).
2. K. H. Row and Y. Jin, *Bioresour. Technol.*, **97**(5), 790 (2006).
3. R. Van Kaam, I. Rodriguez-Donis and V. Gerbaud, *Chem. Eng. Sci.*, **63**, 78 (2008).
4. H.-J. Kang and J.-H. Kim, *Korean J. Chem. Eng.*, **36**(12), 1965 (2019).
5. J. Gmehling, J. Menke, J. Krafczyk, K. Fischer, J.-C. Fontaine and H. V. Kehiaian, Fluid properties. in: *Handbook of chemistry and physics*, 92th Ed., CRC Press, Boca Raton (2005).
6. J. A. Dean, Physical properties. *Lange's handbook of chemistry*, 15th Ed., McGraw-Hill, New York (1999).
7. P. Langston, N. Hilal, S. Shingfield and S. Webb, *Chem. Eng. Process.*, **44**, 345 (2005).
8. Y. Wang, G. Bu, Y. Wang, T. Zhao, Z. Zhang and Z. Zhu, *Comput. Chem. Eng.*, **95**, 97 (2016).
9. E. Hosgor, T. Kucuk, I. N. Oskal and D. B. Kaymak, *Comput. Chem. Eng.*, **67**, 166 (2014).
10. Z. Lei, B. Chen and Z. Ding, *Special distillation processes*, Elsevier, Amsterdam (2005).
11. Q. Li, L. Cao, Y. Zhang, P. Liu and B. Wang, *J. Chem. Eng. Data*, **59**, 234 (2014).
12. T. Hiaki, K. Kurihara and K. Kojima, *J. Chem. Eng. Data*, **39**, 714 (1994).
13. I. I. Vasil'eva, A. N. Marinichev and M. P. Susarev, *Deposited Doc. VINITI*, 3400-83 (1983).
14. I. Nagata, *J. Chem. Eng. Data*, **7**, 367 (1962).
15. A. M. Fulgueras, D. S. Kim and J. Cho, *Korean J. Chem. Eng.*, **33**(1), 46 (2016).
16. J. Lee, J. Cho, D. M. Kim and S. Park, *Korean J. Chem. Eng.*, **28**(2), 591 (2011).
17. X. Gao, X. Yin, S. Yang and D. Yang, *Korean J. Chem. Eng.*, **36**(1), 77 (2019).
18. W. L. Luyben and I. Chien, *Design and control of distillation systems for separating azeotropes*, Hoboken, New Jersey (2010).
19. W. L. Luyben, *Distillation design and control using aspen simulation*, 2nd Ed., Hoboken, New Jersey (2013).
20. J. Cho and J.-K. Jeon, *Korean J. Chem. Eng.*, **23**(1), 1 (2006).

Supporting Information

Separation of methanol-chloroform mixture using pressure-swing distillation: Modeling and optimization

Russel J. Galanido, Dong Sun Kim, and Jungho Cho†

Chemical Process Research Laboratory, Department of Chemical Engineering, Kongju National University, 275 Budae-dong, Cheonan-si, Seobuk-gu, Chungcheongnam-do 31080, Korea
(*Received 25 November 2019 • accepted 31 January 2020*)

Initial No. of Stages and Feed Tray Location

As for column specification such as number of stages and feed tray location, it is more convenient to estimate it based on calculated Fenske minimum trays in PRO/II - Shortcut Column and/or by using McCabe-Thiele method for minimum trays determination. Fig. 1 depicts the minimum tray determination for low- and high-pressure columns using McCabe-Thiele method, while Table 2 tabulates the calculated Fenske for low- and high-pressure columns in PRO/II - Shortcut column.

Suggested no. of trays/stages can be calculated by doubling the Fenske min. no. of trays [18,19]. However, in this study, these suggested no. of stages were used as the new minimum trays basis for column optimization. For convenience, the feed/recycle streams were set at 13th stage for both columns and it was assumed that these streams are at the middle stage of the total column stages. Thus, initial total column stages should be assumed as 25 for both columns.

Number of Theoretical Stages Optimization

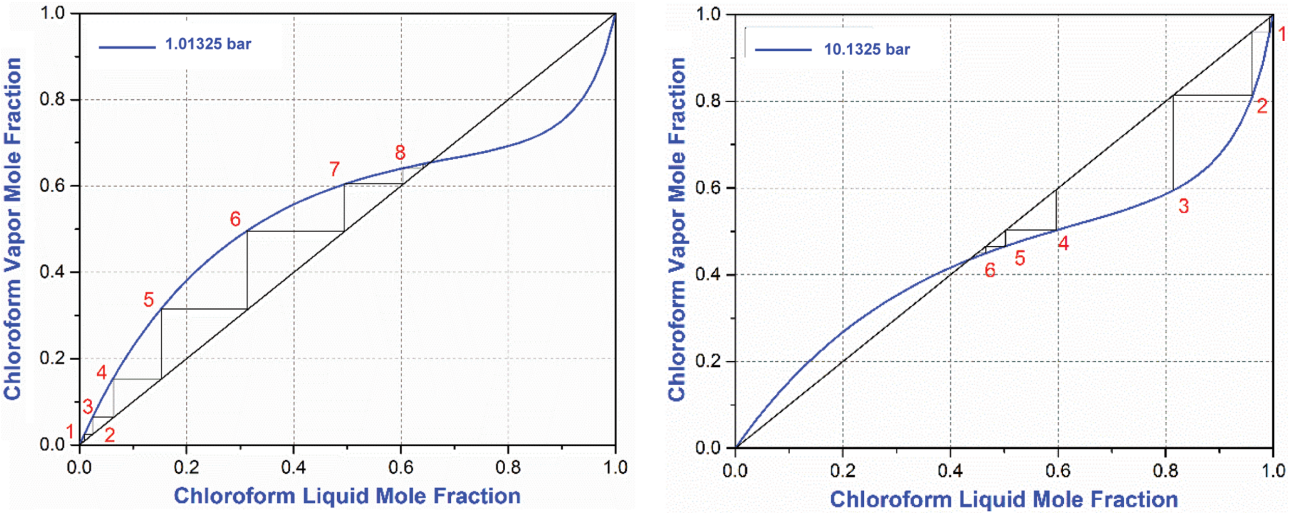


Fig. S1. Minimum tray determination using McCabe-Thiele method.

Table S1. Calculated Fenske minimum trays in PRO/II

Column	Min. No. of Trays	Suggested No. of Trays
Low-pressure	8.6659	17.3318~**18**
High-pressure	6.0671	12.1342~**13**

Table S2. (a) No. of theoretical stages (N) and reflux ratio (RR) relationship for LP column (C-101) using LP+HP configuration

RR	N	RR	N	RR	N
79.8118	13	0.4611	21	0.3729	29
29.2268	14	**0.4134**	**22**	0.3720	30
11.0793	15	0.3923	23	0.3659	40
4.5737	16	0.3831	24	0.3623	50
2.1745	17	0.3789	25	0.3599	60
1.2079	18	0.3765	26	0.3582	70
0.7733	19	0.3750	27	0.3570	80
0.5635	20	0.3739	28	N/A	81+

*Min. RR=0.3750 Required RR=1.2×0.3570=0.4284

Table S2. (b) No. of theoretical stages (N) and reflux ratio (RR) relationship for HP column (C-102) using LP+HP configuration

RR	N	RR	N
15.5005	13	0.5456	21
2.6343	14	0.5456	22
0.7974	15	0.5456	24
0.6255	**16**	0.5456	25
0.5730	17	0.5456	30
0.5534	18	0.5456	35
0.5474	19	0.5456	40
0.5458	20	0.5456	50

*Min. RR=0.5456 Required RR=1.2×0.5456=0.6547

Table S2. (c) No. of theoretical stages (N) and reflux ratio (RR) relationship for HP column (C-201) using HP+LP configuration

RR	N	RR	N
15.5005	13	0.4744	21
2.5509	14	0.4742	22
0.7596	15	0.4742	23
0.6021	16	0.4742	24
0.5306	**17**	0.4742	25
0.4946	18	0.4742	26
0.4805	19	0.4742	27
0.4758	20	0.4742	28

*Min. RR=0.4742 Required RR=1.2×0.4742=0.5690

Table S2. (d) No. of theoretical stages (N) and reflux ratio (RR) relationship for LP column (C-202) using HP+LP configuration

RR	N	RR	N	RR	N
79.9216	13	0.6112	21	0.4828	45
29.3124	14	**0.5504**	**22**	0.4815	50
11.1993	15	0.5202	23	0.4794	60
4.7355	16	0.5057	24	0.4780	70
2.3594	17	0.4986	25	0.4769	80
1.3958	18	0.4899	30	0.4761	90
0.9524	19	0.4868	35	0.4755	100
0.7285	20	0.4845	40	N/A	100+

*Min. RR=0.4755 Required RR=1.2×0.4755=0.5706